

Available online at [www.sciencedirect.com](http://www.sciencedirect.com)

journal homepage: [www.elsevier.com/locate/ajps](http://www.elsevier.com/locate/ajps)

## Original Research Paper

# Characterization and *in vitro* release studies of oral microbeads containing thiolated pectin–doxorubicin conjugates for colorectal cancer treatment

Kamonrak Cheewatanakornkool <sup>a,b</sup>, Sathit Niratisai <sup>c</sup>,  
Somkamol Manchun <sup>b,d</sup>, Crispin R. Dass <sup>e,f</sup>, Pornsak Sriamornsak <sup>a,b,\*</sup>

<sup>a</sup> Department of Pharmaceutical Technology, Faculty of Pharmacy, Silpakorn University, Nakhon Pathom 73000, Thailand

<sup>b</sup> Pharmaceutical Biopolymer Group (PBiG), Faculty of Pharmacy, Silpakorn University, Nakhon Pathom 73000, Thailand

<sup>c</sup> Department of Pharmaceutical Chemistry, Faculty of Pharmacy, Silpakorn University, Nakhon Pathom 73000, Thailand

<sup>d</sup> Thailand Institute of Scientific and Technological Research, Klong Luang, Pathum Thani 12120, Thailand

<sup>e</sup> School of Pharmacy, Faculty of Health Sciences, Curtin University, Perth, WA 6845, Australia

<sup>f</sup> Curtin Health Institute for Research Innovation, Curtin University, Perth, WA 6845, Australia

## ARTICLE INFO

## Article history:

Received 15 June 2017

Accepted 6 July 2017

Available online 12 July 2017

## Keywords:

Microbeads

Thiolated pectin

Doxorubicin

Conjugate

Colorectal cancer

## ABSTRACT

Novel oral microbeads were developed based on a biopolymer–drug conjugate of doxorubicin (DOX) conjugated with thiolated pectin via reducible disulfide bonds. The microbeads were fabricated by ionotropic gelation with cations such as  $Al^{3+}$ ,  $Ca^{2+}$  and  $Zn^{2+}$ . The results showed that using zinc acetate can produce the strongest microbeads with spherical shape. However, the microbeads prepared from thiolated pectin–DOX conjugate were very soft and irregular in shape. To produce more spherical microbeads with suitable strength, the native pectin was then added to the formulations. The particle size of the microbeads ranged from 0.87 to 1.14  $\mu m$ . The morphology of the microbeads was characterized by optical and scanning electron microscopy. DOX was still in crystalline form when used in preparing the microbeads, as confirmed by powder X-ray diffractometry. Drug release profiles showed that the microbeads containing thiolated pectin–DOX conjugate exhibited reduction-responsive character; in reducing environments, the thiolated pectin–DOX conjugate could uncouple resulting from a cleavage of the disulfide linkers and consequently release the DOX. The best-fit release kinetics of the microbeads containing thiolated pectin–DOX conjugate, in the medium without reducing agent, fit the Korsmeyer–Peppas model while those in the medium with reducing agent fit a zero-order release model. These results suggested that the microbeads containing thiolated pectin–DOX conjugate may be a promising platform

\* Corresponding author. Department of Pharmaceutical Technology, Faculty of Pharmacy, Silpakorn University, Nakhon Pathom 73000, Thailand. Tel.: + 66 3425 5800.

E-mail address: [sriamornsak\\_p@su.ac.th](mailto:sriamornsak_p@su.ac.th) (P. Sriamornsak).

Peer review under responsibility of Shenyang Pharmaceutical University.

<https://doi.org/10.1016/j.ajps.2017.07.005>

1818-0876/© 2017 Shenyang Pharmaceutical University. Production and hosting by Elsevier B.V. This is an open access article under the CC BY-NC-ND license (<http://creativecommons.org/licenses/by-nc-nd/4.0/>).

for cancer-targeted delivery of DOX, exploiting the reducing environment typically found in tumors.

© 2017 Shenyang Pharmaceutical University. Production and hosting by Elsevier B.V. This is an open access article under the CC BY-NC-ND license (<http://creativecommons.org/licenses/by-nc-nd/4.0/>).

## 1. Introduction

Colorectal cancer (CRC) is the third most common cancer in the world, with nearly 1.4 million new cases diagnosed in 2012 [1]. Treatments used for CRC include some combination of surgery, radiation therapy and chemotherapy [2,3]. Surgery is the primary treatment for patients affected with potentially curable followed by adjuvant therapy, often suitable in the initial stages; the majority of patients undergo recurrences and metastases. This phenomenon frequently correlates with an acquired resistance to conventional therapies such as chemo- and radiotherapy [2,3]. In metastatic cancer, chemotherapy represents the first-line treatment with the goal of prolonging survival and improving or maintaining quality of life. Chemotherapeutic drugs, such as doxorubicin (DOX), fluorouracil, cisplatin, leucovorin and mitomycin, are commonly used to kill tumor cells that may have remained and metastasized or spread to other parts of the body after surgery, but all such drugs have side-effects, some of them quite serious [2].

DOX, an anthracycline antibiotic (Fig. 1), has been used for decades for treatment of various types of cancers [4–8]. While providing a cure in a good degree of cases, DOX is toxic to most major organs, especially the heart, which renders the treatment dose-limiting [6]. For this reason, many researchers have designed and developed strategies capable of restricting the toxicity of DOX, to aim its effects directly at the tumor as much as possible. Promising drug delivery systems include the entrapment of drugs into polymeric drug carriers, such as hydrogels, nanoparticles, and liposomes [7]. Recently, stimuli-responsive drug delivery systems that deliver a drug in response to specific stimuli, either exogenous (variations in temperature, magnetic field) or endogenous (changes in pH, enzyme concentration or redox gradients), have become possible [9]. Joo and co-workers [10] used pH-responsive DOX–fibrinogen microspheres for tumor-specific drug delivery by conjugating

DOX to fibrinogen via arginine–glycine–aspartate peptide sequences. They found that the drug can be released under mild acidic conditions, and the microspheres have low cytotoxicity to normal cells and high antitumor effect toward cancer cells. Manchun and co-workers [3] developed pH-responsive dextrin nanogels as anticancer drug carriers with pH-controlled drug release. They also found that the anticancer efficacy of DOX is increased by using pH-responsive dextrin nanogels. Vong and Nagasaki [11] attempted an intraperitoneal treatment of murine colon cancer with pH-responsive and redox-responsive nanoparticles containing DOX. The developed nanoparticles could inhibit cancer growth and prolong mice lifespan with low adverse effects.

Redox-responsiveness is one of the frequently adopted strategies for fabricating stimuli-responsive drug delivery vehicles. Reducing substances, such as glutathione (GSH), are widely distributed in the human body and present at higher levels in tumor intracellular environments [12]. The GSH level in tumor cells has been found to be at least four times higher than in normal cells. Due to its reducibility, GSH mediates disulfide bond (S–S) cleavage reactions, through a dithiol–disulfide exchange process [13]. Upon cleavage, it may lead to the disassembly of polymeric backbone materials. This phenomenon provides an opportunity for triggered-release of drug molecules from disulfide-linked polymer–drug conjugates within the tumor cells [14–16]. Su and co-workers [16] have used this advantage to develop stearic acid-grafted chitosan oligosaccharide–DOX conjugates synthesized via disulfide linkers. The polymer–drug conjugates exhibited good anti-tumor efficacy, selective accumulation in tumor and reduced accumulation in the heart. Yang and co-workers [17] developed redox/pH dual stimuli-responsive PEGylated polymeric micelles for intracellular DOX delivery. DOX can be selectively released in response to a lower intracellular pH of 5.0 (endosomal pH) and a higher reducing environment, demonstrating redox/pH-responsive controlled drug release capability.

Oral administration is one of the most accepted and simple modes of drug delivery. In general, oral administration has several benefits such as non-invasive administration, higher patient compliance, self-administration, and cost reduction. Only in the treatment of hematological and central nervous system tumors, it has been widely accepted, but in the case of other tumors, it remains an exception [18]. A number of reasons may justify the low introduction of oral compounds; the most important limitation of oral chemotherapy is probably the concern around its bioavailability and potential side-effect [19,20]. Designing and formulating an oral dosage form for a chemotherapeutic agent through the GI tract requires a number of carefully considered strategies. Drug release should be suppressed in the stomach and small intestine. Sahoo et al. [20] prepared gellan gum microbeads containing fluorouracil

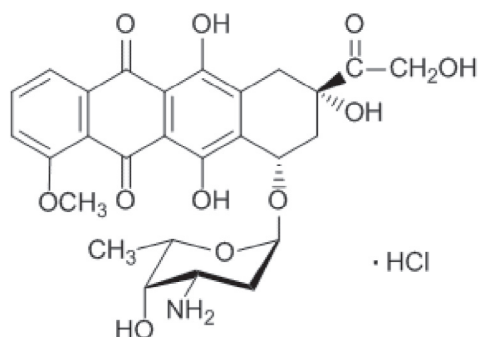


Fig. 1 – Chemical structure of doxorubicin (DOX).

for oral administration by simple ionotropic gelation. They found that gellan gum or gellan gum/ethyl cellulose microbeads led to sustained release of drug and prolonged tumor cell kill. Recently, DOX was encapsulated in microbeads composed of alginate–carboxy methyl guar gum for oral controlled delivery [21]. No DOX release from the microbeads at pH 1.2 was detected; however, 16% DOX was released from the microbeads at pH 7.4 within 8 h.

In the current study, pectin was used as a gel-forming polymer for fabricating oral microbeads. In fact, pectin, a polysaccharide found in the cell walls of most plants [22], has long been used to prepare gel beads for oral delivery of various drugs to different parts of the GI tract [23–26]. Pectin beads have also been used as a carrier for colon-specific drug delivery system [27,28] as it is selectively digested by colonic microflora to release drug with minimal degradation in the upper GI tract [29]. Chemically, pectin consists of the partial methyl esters of polygalacturonic acid and their salts, with a molecular weight of up to 150 kDa. Pectin is usually classified according to the degree of methoxylation (DM), a percentage of esterified galacturonic acid units to total galacturonic acid units in the molecules of pectin. Pectin containing more than 50% of methoxyl groups is classified as high methoxyl pectin (HMP) while that containing less than 50% methoxyl groups is classified as low methoxyl pectin (LMP).

The purpose of the current study was, therefore, to fabricate novel microbeads containing pectin and thiolated pectin–DOX conjugates, by simple ionotropic gelation technique, for the future purpose of anticancer drug delivery to the colon via oral administration. The morphology of microbeads was characterized by scanning electron microscopy (SEM). Particle size, drug crystallinity, drug content in the microbeads, and *in vitro* drug release were also investigated.

## 2. Materials and methods

### 2.1. Materials

Low methoxy pectin (type CU701, lot number 00412079) with DE of 38% and high methoxy pectin (type CU201, lot number 00501087) with DE of 70% were obtained from Herbstreith & Fox AG, Germany. Cystamine dihydrochloride (lot number BCBL6131V) was purchased from Fluka Analytical, Switzerland. Thioglycolic acid (98%) for synthesis (lot number S5678863411) and *N*-hydroxysuccinamide (NHS) (lot number A0266926) were from Merck KGaA (Germany) and ACROS Organic (USA), respectively. *L*-Cysteine hydrochloride (lot number BCBM8363V), 3,3'-dithiopropionic acid (lot number MKBL7043V), 5,5'-dithio-bis-(2-nitrobenzoic acid) (lot number MCFD00007140), *N*-(3-dimethylaminopropyl)-*N*-ethylcarbodiimide hydrochloride (EDC) (lot number 037K0753), *DL*-dithiothreitol (DTT) (lot number SLBK 4951V), and DOX (hydrochloride salt) (lot number SLB 1340V) were purchased from Sigma-Aldrich Co., Ltd. (MO, USA). Ethylene diamine tetraacetic acid disodium salt dehydrate (EDTA) (lot number J069H11) and zinc acetate (lot number 1501186173) were purchased from Rankem, Ltd. (India) and Ajax Finechem (Australia), respectively. All other chemicals used were of reagent grade or analytical grade.

### 2.2. Preparation of thiolated pectin–doxorubicin conjugates

The thiolated pectin–DOX conjugates were synthesized by two methods, that is, disulfide bond formation reaction and disulfide bond exchange reaction, as reported in previous work [30]. The synthesis of thiolated pectin–DOX conjugate by disulfide bond formation reaction includes three steps. First, DOX was dissolved in cold distilled water, followed by the addition of EDC, NHS, and 3,3'-dithiopropionic acid, to obtain DOX–3,3'-dithiopropionic acid conjugate. After stirring for 2 h, DTT was then added dropwise and the reaction was continued for 2 h. Second, thiolated pectin (both HMP and LMP) was synthesized by dissolving pectin in warm water; cystamine dihydrochloride, EDC and NHS were added in the reaction. DTT and hydrogen peroxide were added to the thiolated pectin solution. Third, thiolated pectin with thiol terminal obtained was added to the stirred solution of DOX–3,3'-dithiopropionic acid conjugate with thiol terminal. The product of thiolated pectin–DOX conjugate obtained was purified by dialysis against distilled water for 72 h and then lyophilized (model Freezone 2.5, Labconco, USA) under 0.29 mbar and  $-49^{\circ}\text{C}$ .

The synthesis steps for thiolated pectin–DOX conjugate by disulfide bond exchange reaction were similar to that by disulfide bond formation reaction, except no thiol terminal groups were formed. First, the DOX–3,3'-dithiopropionic acid conjugate was synthesized and adjusted to basic pH by triethylamine, as mentioned above. Subsequently, the thiolated pectin solution was poured into the mixture and stirred for 6 h. The product of thiolated pectin–DOX conjugate obtained was purified and lyophilized in the same manner as mentioned above.

### 2.3. Microbead preparation

The microbeads containing thiolated pectin–DOX conjugates were fabricated by a simple ionotropic gelation technique [31–33]. Various cross-linking agents, namely calcium chloride ( $\text{CaCl}_2$ ), aluminum chloride ( $\text{AlCl}_3$ ), zinc chloride ( $\text{ZnCl}_2$ ) and zinc acetate ( $\text{Zn}(\text{OAc})_2$ ), were used in this study. The lyophilized thiolated pectin–DOX conjugate was dissolved in distilled water and then mixed with the solution of native (raw material) pectin. The final concentration of native pectin is 2% (w/w). The mixture solution was extruded dropwise, through a 27-gauge needle, into cross-linking solution with continuous stirring at room temperature for 20 min. The gel beads formed were filtered and washed 3 times with distilled water, put on a polytetrafluoroethylene tray, and then dried at room temperature for 12 h and in a hot-air oven at  $40^{\circ}\text{C}$  for another 2 h. Fig. 2 depicts the microbead preparation procedure using an ionotropic gelation method. The microbeads were kept in a desiccator until used.

### 2.4. Powder X-ray diffractometry (PXRD)

PXRD patterns of DOX and the microbeads were determined by powder X-ray diffractometer (model Miniflex II, Rigaku, Japan), at 15 mA, 30 kV and angle speed of  $4^{\circ}/\text{min}$  over the range of  $2\theta$  from  $5$  to  $45^{\circ}$ , using  $\text{Cu K}\alpha$  radiation wavelength of  $1.5406 \text{ \AA}$ .

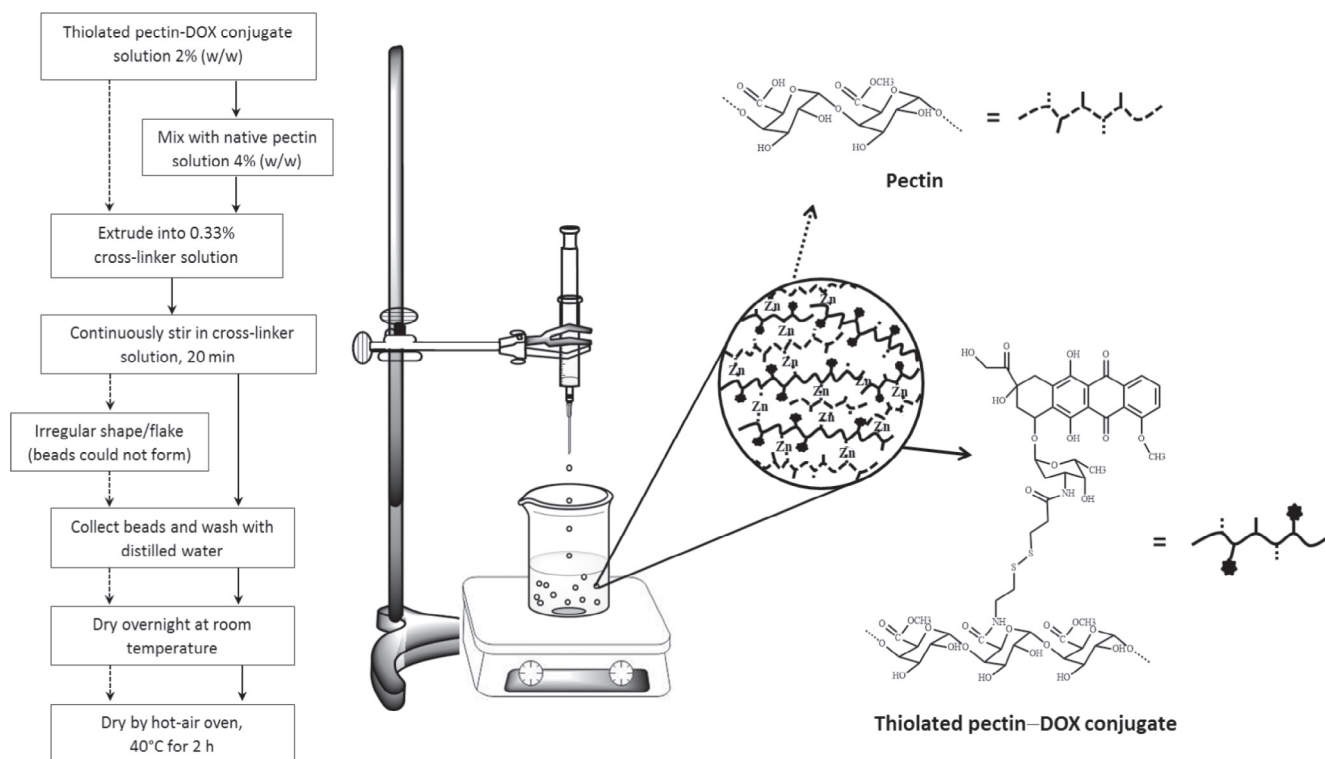


**Fig. 2 – Ionotropic gelation method for preparation of microbeads containing thiolated pectin–DOX conjugates.**

## 2.5. Morphology and particle size determination

Surface morphology of the microbeads containing thiolated pectin–DOX conjugates was carried out using scanning electron microscopy (SEM; model Maxim-2000, CamScan Analytical, England), operating at an acceleration voltage of 15 kV. All samples were fixed on SEM stubs with double-sided adhesive tape and then coated in a vacuum with thin gold layer before investigation.

The light microscope (model IX51, Olympus, Japan) was also used to determine the particle size and shape of the microbeads. The images were captured and processed by ImageJ software (National Institutes of Health, USA).

## 2.6. Drug content determination

The drug content of the microbeads containing thiolated pectin–DOX conjugates was determined after extracting DOX from the microbeads. The samples were dissolved into phosphate buffer, pH 7, containing 0.25 M EDTA and 0.01 M DTT. The mixture was continuously stirred for 4 h (protection from light) and then filtered through 0.22- $\mu$ m filter. The DOX content was determined by fluorescence spectrometry (model RF 1501, Shimadzu Corporation, Japan). Fluorescence measurement was recorded at an excitation wavelength ( $E_x$ ) of 485 nm and an emission wavelength ( $E_m$ ) of 555 nm. All measurements were performed in triplicate. DOX concentration was then calculated based on a calibration curve of known amounts of DOX in distilled water. DOX content was defined as:

$$\text{DOX content (\%)} = \frac{\text{Actual DOX content in microbeads (mg)} \times 100}{\text{Weight of the microbeads (mg)}} \quad (1)$$

## 2.7. In vitro drug release study

The release profiles of DOX from the microbeads containing thiolated pectin–DOX conjugates were performed using a dialysis method modified from previous reports [34–36]. Briefly, the microbeads with 1-mL distilled water were filled into a dialysis tube (Cellu-Sep® T2, MWCO 6–8 kDa, Membrane Filtration Products Inc., Belgium). The simulation of GI transit conditions was achieved by using different dissolution medium pHs at the specified time interval. The dialysis tube was immersed in the vessel containing 20-ml pH 1.2 simulated gastric fluid (SGF) for the first 2 h, pH 6.8 phosphate buffered saline (PBS) for 2 h and then pH 7.4 PBS for another 6 h. The vessels were shaken at 150 rpm using a shaker-incubator (model ES-20, Biosan, Latvia), maintained at 37 °C. At specified time points, the outside buffer was removed and replaced with fresh buffer. The DOX concentration in the collecting buffer was analyzed via fluorescence spectroscopy as above.

## 2.8. Drug release kinetics

The kinetics of DOX release were computed by fitting the dissolution curve to standard empirical equations, that is, Korsmeyer–Peppas, Higuchi, zero order kinetics and first order kinetics equations [37,38] by using curve fitting software,



KinetDS (<http://kinetds.soft112.com/>) [39]. The data were evaluated according to the following equations:

$$\text{Zero-order model: } M_t/M_\infty = kt \quad (2)$$

$$\text{First-order model: } \ln(1 - (M_t/M_\infty)) = -kt \quad (3)$$

$$\text{Higuchi equation: } M_t/M_\infty = kt^{1/2} \quad (4)$$

$$\text{Korsmeyer–Peppas model: } M_t/M_\infty = kt^n \quad (5)$$

where  $M_t/M_\infty$  is the fraction of drug released at time  $t$  and  $k$  is a constant incorporating structural and geometric characteristics of dosage form. In Eq. (5), the release exponent,  $n$ , characterizes the mechanism of drug release [37,39].

### 2.9. Statistical analysis

Data were analyzed using SPSS version 10.0 for Windows (SPSS Inc., USA). The results were represented as mean  $\pm$  standard deviation (SD). Student's  $t$ -test or analysis of variance (ANOVA) was used to determine the difference among the groups, and pairs were compared using either the Scheffé or Games-Howell test. The statistical significance was set at  $P < 0.05$ .

## 3. Results and discussion

### 3.1. Fabrication of microbeads containing thiolated pectin–DOX conjugates

The microbeads containing thiolated pectin–DOX conjugates were fabricated by ionotropic gelation method using various cross-linking agents. When the aqueous dispersion of pectin or thiolated pectin–DOX conjugates was extruded into cross-linking solutions ( $\text{Ca}^{2+}$ ,  $\text{Al}^{3+}$  or  $\text{Zn}^{2+}$  counter ions), gelled microbeads were produced instantaneously, according to the so-called “egg-box model” [22,40]. In this process, intermolecular cross-links were formed between negatively-charged carboxyl groups of pectin and positively-charged counter ions [25,27]. Table 1 shows the appearance, firmness and morphology of fresh and dry microbeads prepared from various cross-linking agents. It is observed that the type of cross-linking agent influenced the appearance, firmness and morphology of the microbeads obtained. The fresh microbeads were almost spherical for all cross-linking agents used. However, upon air-drying, the microbeads of all preparations shrank significantly. The microbeads using zinc chloride and aluminum chloride as cross-link agent were insufficiently strong and showed a collapsed structure. The strong association of zinc acetate and calcium chloride resulted in spherical microbeads. The rank order of firmness of the microbeads using different cross-linking agents is as follows: aluminum chloride < zinc chloride < calcium chloride < zinc acetate. It is likely due to the strong association of  $\text{Zn}^{2+}$  to pectin chain. Assifaoui and co-workers [41] suggested that  $\text{Zn}^{2+}$  interacts with both carboxylate and hydroxyl groups of galacturonate units in a similar way to that described in the egg-box model, whereas calcium ions

only interact with carboxylate groups. Therefore, zinc acetate was used for preparing all further batches of microbeads.

### 3.2. Characterization of microbeads containing thiolated pectin–DOX conjugates

#### 3.2.1. Particle size of microbeads

Table 2 presents particle size of microbeads prepared from different pectin samples, which are native pectin, thiolated pectin and thiolated pectin–DOX conjugates. The particle size of microbeads prepared from LMP ranged from 1.01 to 1.15 mm. The size of microbeads prepared from native HMP was  $0.871 \pm 0.077$  mm. Using thiolated HMP–DOX conjugate (prepared by both disulfide bond formation and disulfide bond exchange reaction), the size was  $1.097 \pm 0.129$  mm which is larger (about 10%) than using native HMP.

#### 3.2.2. Powder X-ray diffractometry (PXRD)

PXRD was applied to resolve the sample which can be correlated with the formation of a homogeneous, single phase with a higher apparent solubility than the crystalline/partially crystalline drug [42]. According to previous reports, the PXRD pattern of pure DOX in native form showed sharp distinctive crystalline peaks at  $2\theta$  of 16.6, 19.2, 20.4, 22.4, and 24.9° [42–44] while that of native pectin showed a typical amorphous pattern (data not shown). The PXRD patterns of zinc acetate, microbeads containing native pectin, thiolated pectin, thiolated pectin–DOX conjugate synthesized by disulfide exchange reaction or disulfide formation reaction, compared to that of DOX-loaded microbeads, are shown in Fig. 3. The PXRD peaks associated with the DOX crystal were observed in the DOX-loaded thiolated pectin microbeads, suggesting that the DOX was in native form. From the PXRD patterns of microbeads containing thiolated pectin–DOX conjugate, the characteristic peaks of DOX were still found but in less extent, suggesting that crystalline DOX was not fully phase-transformed to amorphous [42,44]. Moreover, all microbead formulations exhibited the characteristic peaks of zinc acetate at the same  $2\theta$  with standard zinc acetate ( $2\theta$  of 12.9, 16.9, 20.5, 22.8, 25.5 and 28.0°).

#### 3.2.3. Morphology of microbeads

After coupling to DOX, pectin properties were changed slightly. It is suggested that the functionality of pectin depends on the amount of ion-binding groups attached to the polymer [22]. The free carboxyl groups of thiolated pectin were reduced after coupling with DOX, compared to native pectin; the gelation resulted from the ionic interaction between galacturonic residues of pectin backbone and divalent cations was decreased. Therefore, the strength of microbeads fabricated from thiolated pectin was low, resulting in soft microbeads with irregular shape (data not shown). To produce more spherical microbeads with suitable strength, the native pectin was then added to all formulations. Fig. 4 depicts the optical microscopic images of microbeads fabricated from only native pectin, thiolated pectin (plus native pectin) and thiolated pectin–DOX conjugates (plus native pectin). The microbeads fabricated from only native pectin were less spherical than those fabricated from thiolated pectin (plus native pectin) and thiolated pectin–DOX conjugates (plus native pectin). The morphology of microbeads observed by SEM is presented in Fig. 5. The images show that

**Table 1 – Appearance, firmness and morphology of microbeads prepared from various cross-linking agents.**

Cross-linking agent	Appearance	Firmness	Morphology
Fresh beads			
Calcium chloride	Spherical	Medium	
Aluminum chloride	Spherical	Very soft	
Zinc chloride	Spherical/irregular	Soft	
Zinc acetate	Spherical	Hard	
Dry beads			
Calcium chloride	Spherical	Brittle	
Aluminum chloride	Flat	Brittle	
Zinc chloride	Flat	Brittle	
Zinc acetate	Spherical	Hard	

**Table 2 – Particle size of microbeads prepared from different pectin samples.**

Pectin sample	Particle size (mm) $\pm$ SD, n = 15
Native LMP	1.04 $\pm$ 0.07
Thiolated LMP with terminal thiol group	1.11 $\pm$ 0.19
Thiolated LMP with disulfide bond	1.04 $\pm$ 0.13
Thiolated LMP–DOX conjugate (prepared by disulfide bond formation)	1.14 $\pm$ 0.24
Thiolated LMP–DOX conjugate (prepared by disulfide bond exchange)	1.10 $\pm$ 0.07
Native HMP	0.87 $\pm$ 0.08
Thiolated HMP with terminal thiol group	0.93 $\pm$ 0.10
Thiolated HMP with disulfide bond	0.93 $\pm$ 0.09
Thiolated HMP–DOX conjugate (prepared by disulfide bond formation)	1.10 $\pm$ 0.13
Thiolated HMP–DOX conjugate (prepared by disulfide bond exchange)	1.08 $\pm$ 0.11

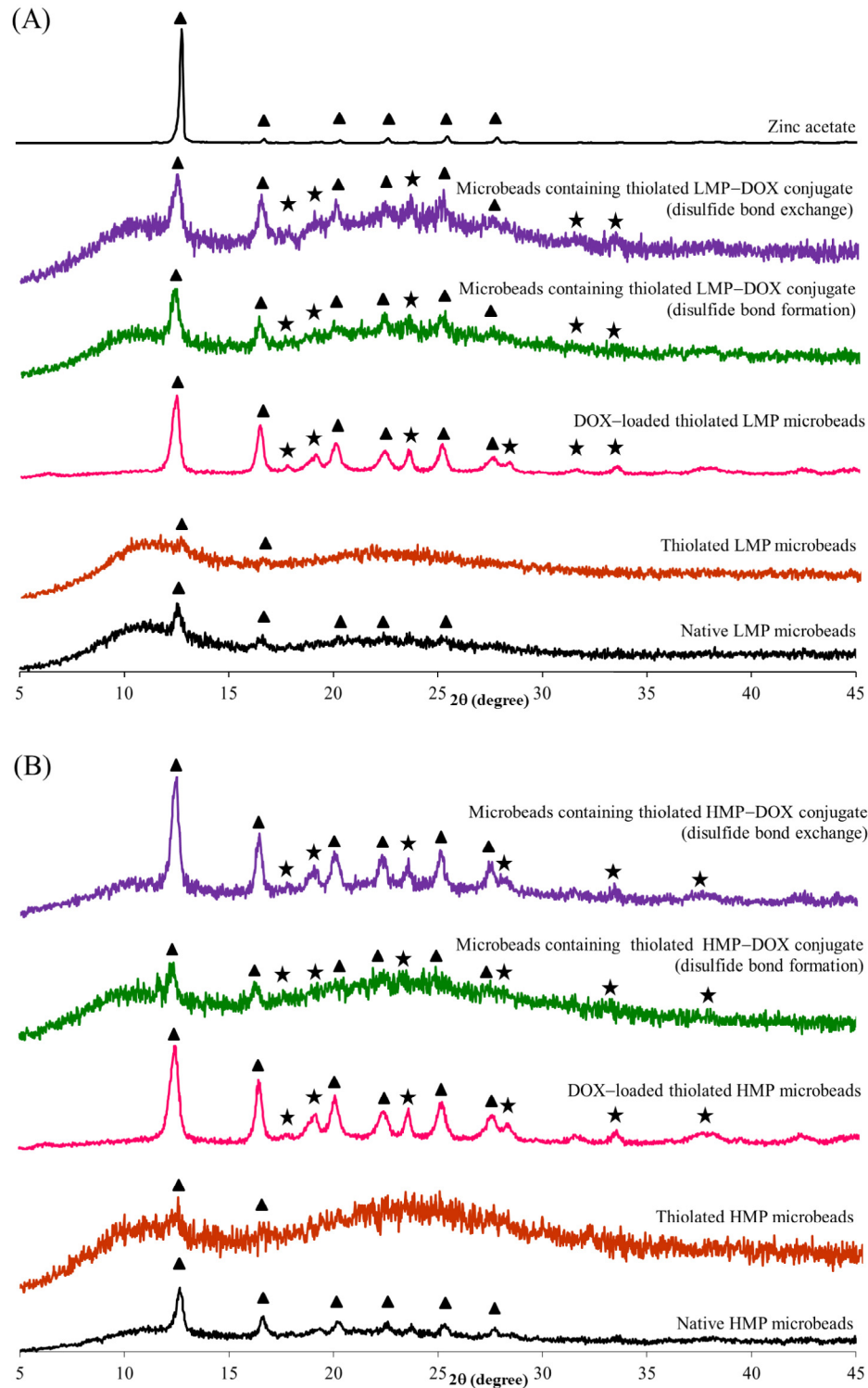


**Fig. 3 – Powder X-ray diffraction (PXRD) patterns of zinc acetate, microbeads containing native pectin, thiolated pectin, thiolated pectin-DOX conjugate synthesized by disulfide exchange reaction or disulfide formation reaction, compared to DOX-loaded microbeads; (A) LMP and (B) HMP. Note: ★ = characteristic peaks of DOX, ▲ = characteristic peaks of zinc acetate.**

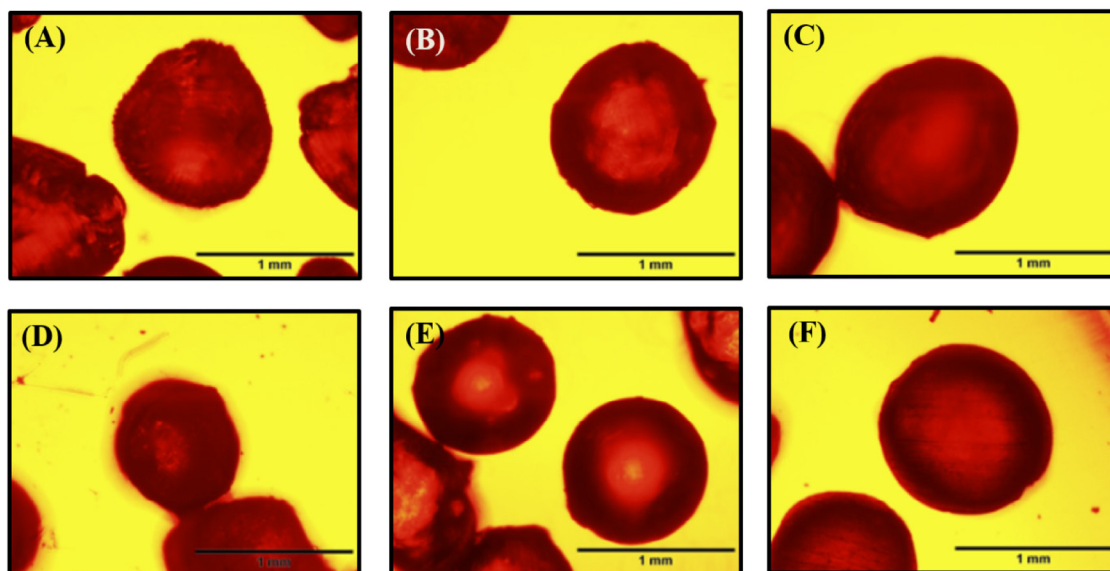


Fig. 4 – Optical microscopic images of microbeads fabricated from (A) native LMP, (B) thiolated LMP plus native LMP, (C) thiolated LMP-DOX conjugate plus native LMP, (D) native HMP, (E) thiolated HMP plus native HMP, (F) thiolated HMP-DOX conjugate plus native HMP; scale bar = 1.0 mm.

the surface of microbeads containing thiolated HMP-DOX conjugate was smoother than that containing thiolated LMP-DOX conjugate. The internal structure of the microbeads was dense and showed no pore (Fig. 5B and D).

### 3.3. Drug content

Table 3 displays DOX content in microbeads containing thiolated pectin-DOX conjugates. The DOX content in microbeads con-

taining thiolated LMP-DOX conjugate was higher than those containing thiolated HMP-DOX conjugate. It is likely that LMP has more carboxylic acid groups available for coupling reaction with DOX. Therefore, a higher amount of DOX can be retained in the structure. It is also obvious that the DOX content in microbeads depended on the conjugation method. The microbeads containing thiolated LMP-DOX conjugate synthesized by disulfide exchange reaction had the highest DOX content, that is,  $906.8 \pm 90.1$  of DOX in 1 g of microbeads, fol-

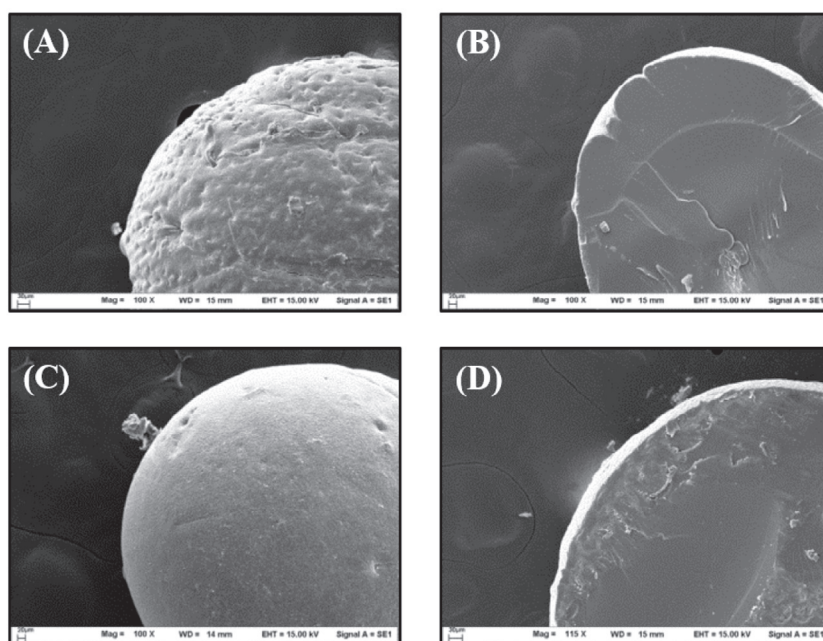


Fig. 5 – SEM images of microbeads containing thiolated pectin-DOX conjugate; (A) surface and (B) cross-section of microbeads containing thiolated LMP-DOX conjugate and (C) surface and (D) cross-section of microbeads containing thiolated HMP-DOX conjugate; at magnification of 100x.



**Table 3 – DOX content in microbeads containing thiolated pectin–DOX conjugates.**

Type of thiolated pectin–DOX conjugate in microbeads	DOX content ( $\mu\text{g/g}$ bead) $\pm$ SD, $n = 3$
Thiolated LMP–DOX conjugate (disulfide bond formation)	681.1 $\pm$ 99.7
Thiolated LMP–DOX conjugate (disulfide bond exchange)	906.8 $\pm$ 90.1
Thiolated HMP–DOX conjugate (disulfide bond formation)	501.8 $\pm$ 54.4
Thiolated HMP–DOX conjugate (disulfide bond exchange)	567.0 $\pm$ 114.4

lowed by those synthesized by disulfide bond formation reaction. Similar results were observed in the case of the microbeads containing thiolated HMP–DOX conjugate. It is suggested that the disulfide exchange reaction had a higher efficiency than the disulfide bond formation reaction. The disulfide exchange reaction required only a few steps for synthesis, which could minimize DOX loss during synthesis.

### 3.4. In vitro drug release

We expected that the presence of disulfide bridges linking between thiolated pectin and DOX should allow a redox-responsive DOX release. The *in vitro* release of DOX from the microbeads was performed under typical GI transit conditions. To demonstrate the responsiveness of our drug delivery system, DTT (at a concentration of 10 mM) was incorporated in order to mimic the tumor environment in the colon. Fig. 6 shows *in vitro* release profiles of DOX from different microbead formulations. The control formulations, DOX-loaded microbeads prepared from thiolated pectins (both LMP and HMP), showed the DOX burst release; almost 60% DOX release were observed within 2 h (Fig. 6B). This is probably due to the small molecular size of the physically entrapped DOX.

The DOX burst release could be reduced when DOX was conjugated with pectin before loading into the microbeads (Fig. 6B). Moreover, the microbeads containing thiolated pectin–DOX conjugate were stable in the upper part of the GI tract (simulated media using pH 1.2 SGF and pH 6.8 PBS). The results in Fig. 6A demonstrate that the microbeads containing thiolated LMP–DOX conjugate exhibited a slower DOX release, in the first 2 h. After that, the release in pH 6.8 buffer was dramatically increased; this phenomenon was influenced by pectin properties. Although the disulfide bond could not be cleaved in the upper GI tract, some DOX release from the microbeads was observed. This probably resulted from the other bonds formed during synthesis of thiolated pectin–DOX conjugate, for example, amide

bond, ionic bond, hydrazone bond or ester bond that can be broken easily by hydrolysis under acidic conditions [45–47].

In the presence of 10 mM DTT, the release of DOX from microbeads containing thiolated pectin–DOX conjugate was significantly higher than the release in the medium without DTT ( $P < 0.05$ ). These results confirmed the redox-responsive properties of the microbeads containing thiolated pectin–DOX conjugate. In theory, DOX should not be released from the microbeads containing thiolated pectin–DOX conjugate in the medium without a reducing agent. However, in the synthesis process, other non-specific bonds (as mentioned above) may have formed, resulting in unwanted DOX release. These observations agreed well with previous reports [45,47], which suggested that the polymer and DOX are linked through a degradable amide bond that can be hydrolyzed under acidic conditions. From these results, it is not surprising that the thiolated pectin–DOX conjugate released DOX rapidly in response to a redox environment.

### 3.5. Drug release kinetics

Release kinetic models can be used to describe the overall release of drug from the dosage forms. The changes in a formulation may alter drug release and *in vivo* performance. *In vitro* drug release data can be used to some extent to predict *in vivo* performance in the development of controlled release formulations. Model dependent methods (zero-order, first-order, Higuchi and Korsmeyer–Peppas models) can be used to investigate the kinetics of drug release from controlled release formulations. In order to investigate the drug-release kinetics, release data of DOX were fitted to various kinetic models such as zero-order, first-order, Higuchi equation, and Korsmeyer–Peppas equation. Table 4 shows the mathematical modeling and drug release kinetics from microbeads, analyzed by regression coefficient method. A correlation coefficient ( $R^2$ ) was chosen to define the approximation accuracy of an

**Table 4 – Mathematic modeling and drug release kinetics from microbeads, analyzed by regression coefficient method.**

Formulation	Zero order $R^2$	First order $R^2$	Higuchi $R^2$	Korsmeyer–Peppas	
				$R^2$	$n$
<b>Medium without reducing agent</b>					
Microbeads containing thiolated HMP–DOX conjugate	0.938	0.838	0.471	0.974 <sup>a</sup>	0.87
Microbeads containing thiolated LMP–DOX conjugate	0.948	0.648	0.762	0.976 <sup>a</sup>	0.85
<b>Medium with reducing agent (DTT)</b>					
Microbeads containing thiolated HMP–DOX conjugate	0.980 <sup>a</sup>	0.825	0.816	0.973	0.67
Microbeads containing thiolated LMP–DOX conjugate	0.926 <sup>a</sup>	0.879	0.677	0.792	0.58
DOX-loaded thiolated HMP microbeads	0.827	0.570	0.909	0.942 <sup>a</sup>	0.56
DOX-loaded thiolated LMP microbeads	0.839	0.765	0.917	0.956 <sup>a</sup>	0.44

<sup>a</sup> The highest correlation coefficient ( $R^2$ ), compared to other models.

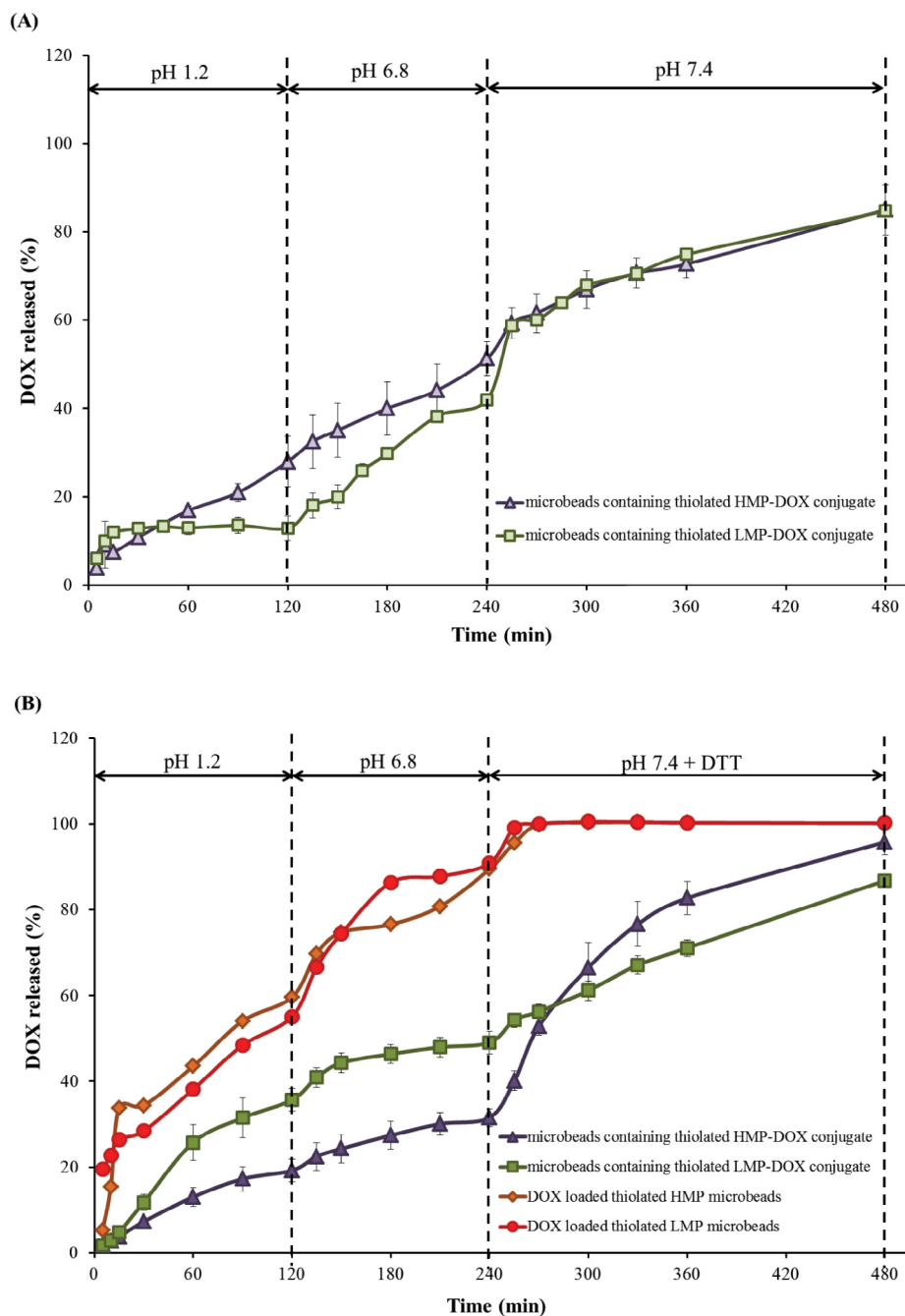


**Fig. 6 – In vitro release profiles of DOX from different microbead formulations; (A) in simulated release media without reducing agent, DTT, and (B) in simulated release media with 10-mM DTT.**

individual model. In the medium without DTT, the Korsmeyer–Peppas model showed higher  $R^2$  values for both microbeads containing thiolated HMP–DOX conjugate and thiolated LMP–DOX conjugate than other models. The Korsmeyer–Peppas model has been used very often to describe the drug release from several different modified-release dosage forms. There are several simultaneous processes considered in this model, for example, diffusion of water into the microbeads, swelling of the microbeads as water entered, formation of gel, diffusion of drug out of the microbeads, and dissolution of the polymer matrix. In this model, the mechanism of drug release is char-

acterized using the release exponent (“ $n$ ” value). For a spherical particle, an “ $n$ ” value of 0.85 corresponds to zero-order release kinetics (case II transport);  $0.43 < n < 0.85$  means an anomalous (non-Fickian) diffusion release model;  $n = 0.43$  indicates Fickian diffusion, and  $n > 0.85$  indicates a super case II transport relaxational release [37,38]. The results revealed that the microbeads containing thiolated HMP–DOX conjugate and thiolated LMP–DOX conjugate obeyed case II transport (zero-order release kinetics), since they fitted well with the Korsmeyer–Peppas model ( $R^2$  is in range of 0.974–0.976 and  $n$  value close to 0.85).

The DOX release kinetics in the medium with DTT showed different results. For the microbeads containing thiolated HMP–DOX conjugate and thiolated LMP–DOX conjugate, a biphasic release profile was observed. The initial slow drug leakage, nearly linear behavior, was found in the first 4 h (in pH 1.2 SGF, followed by pH 6.8 buffer). For the remaining time, after the reducing agent was added, a burst release was observed. Zero-order release model was found to be the best fitted model for these formulations. The release of DOX followed the non-Fickian release mechanism with  $n$  value varying from 0.58 to 0.67, suggesting a combination of diffusion and swelling effects. However, the best-fit release kinetics for the DOX-loaded thiolated HMP and LMP microbeads was achieved with Korsmeyer–Peppas model ( $R^2$  of 0.926–0.980); the DOX release followed the non-Fickian release mechanism with  $n$  value varying from 0.44 to 0.56. The release from DOX-loaded microbeads was also suited to the Higuchi model, with  $R^2$  of 0.909–0.917, suggesting the release controlled by diffusion.

#### 4. Conclusion

The oral microbeads containing thiolated pectin–DOX conjugate were fabricated by an ionotropic gelation method using various cations. Zinc acetate produced the strongest microbeads with spherical shape. The microbeads prepared from thiolated pectin–DOX conjugate were, however, very soft and have irregular shape. When native pectin was added to the formulations, more spherical microbeads with suitable strength were obtained. Drug release profiles showed that the microbeads containing thiolated pectin–DOX conjugate exhibited reduction-responsive behavior. The thiolated pectin–DOX conjugate could uncouple under reducing environments, resulting from a cleavage of the disulfide linkers, and release the DOX. The best-fit release kinetics of the microbeads containing thiolated pectin–DOX conjugate, in the medium with reducing agent, was achieved with zero-order release model. The study indicated the suitability of microbeads containing thiolated pectin–DOX conjugate in delivering DOX via oral administration.

#### Conflicts of interest

The authors declare that there are no conflicts of interest.

#### REFERENCES

- [1] Torre LA, Bray F, Siegel RL, et al. Global cancer statistics, 2012. *CA Cancer J Clin* 2015;65:87–108.
- [2] Labianca R, Beretta GD, Kildani B, et al. Colon cancer. *Crit Rev Oncol Hematol* 2010;74:106–133.
- [3] Manchun S, Dass CR, Cheewatanakornkool K, et al. Enhanced anti-tumor effect of pH-responsive dextrin nanogels delivering doxorubicin on colorectal cancer. *Carbohydr Polym* 2015;126:222–230.
- [4] Minotti G, Menna P, Salvatorelli E, et al. Anthracyclines: molecular advances and pharmacologic developments in antitumor activity and cardiotoxicity. *Pharmacol Rev* 2004;56:185–229.
- [5] Menna P, Salvatorelli E, Minotti G. Doxorubicin degradation in cardiomyocytes. *J Pharmacol Exp Ther* 2007;322:408–429.
- [6] Lyu YL, Liu LF. Doxorubicin cardiotoxicity revisited: ROS versus Top2. In: Liu XY, Pestka S, Shi YF, editors. *Recent advances in cancer research and therapy*. Oxford: Elsevier; 2012. p. 351–369.
- [7] Tacar O, Sriamornsak P, Dass CR. Doxorubicin: an update on anticancer molecular action, toxicity and novel drug delivery systems. *J Pharm Pharmacol* 2013;65:157–170.
- [8] Gutiérrez-Salmeán G, Ceballos G, Meaney E. Anthracyclines and cardiotoxicity. *Int J Cancer Res Prev* 2015;8:515–521.
- [9] Ding C, Tong L, Feng J, et al. Recent advances in stimuli-responsive release function drug delivery systems for tumor treatment. *Molecules* 2016;21:1715.
- [10] Joo JY, Park GY, An SSA. Biocompatible and biodegradable fibrinogen microspheres for tumor-targeted doxorubicin delivery. *Int J Nanomedicine* 2015;10:101–111.
- [11] Vong LB, Nagasaki Y. Combination treatment of murine colon cancer with doxorubicin and redox nanoparticles. *Mol Pharm* 2016;13:449–455.
- [12] Teo JY, Chin W, Ke X, et al. pH and redox dual-responsive biodegradable polymeric micelles with high drug loading for effective anticancer drug delivery. *Nanomedicine* 2017;13:431–442.
- [13] Cheng R, Feng F, Meng F, et al. Glutathione-responsive nano-vehicles as a promising platform for targeted intracellular drug and gene delivery. *J Control Release* 2011;152:2–12.
- [14] Xu H, Ma H, Yang P, et al. Targeted polymer-drug conjugates: current progress and future perspective. *Colloids Surf B Biointerfaces* 2015;136:729–734.
- [15] Wen H, Li Y. Redox sensitive nanoparticles with disulfide bond linked sheddable shell for intracellular drug delivery. *J Med Chem* 2014;4:748–755.
- [16] Su Y, Hu Y, Du Y, et al. Redox-responsive polymer–drug conjugates based on doxorubicin and chitosan oligosaccharide-g-stearic acid for cancer therapy. *Mol Pharm* 2015;12:1193–1201.
- [17] Yang HY, Jang MS, Gao GH, et al. Construction of redox/pH dual stimuli-responsive PEGylated polymeric micelles for intracellular doxorubicin delivery in liver cancer. *Polym Chem* 2016;7:1813–1825.
- [18] Mei L, Zhang Z, Zhao L, et al. Pharmaceutical nanotechnology for oral delivery of anticancer drugs. *Adv Drug Deliv Rev* 2013;65:880–890.
- [19] Battle JF, Arranz EE, Carpeño JC, et al. Oral chemotherapy: potential benefits and limitations. *Clin Transl Oncol* 2004;6:335–340.
- [20] Sahoo SK, Sahoo SK, Behera A, et al. Formulation, in vitro drug release study and anticancer activity of 5-fluorouracil loaded gellan gum microbeads. *Acta Pol Pharm* 2013;70:123–127.
- [21] Bosio VE, Lopez AG, Mukherjee A, et al. Tailoring doxorubicin sustainable release from biopolymeric smart matrix using congo red as molecular helper. *J Mater Chem B* 2014;2:5178–5186.
- [22] Sriamornsak P. Chemistry of pectin and its pharmaceutical uses: a review. *Silpakorn Univ Int J* 2003;3:206–228.
- [23] Sriamornsak P. Application of pectin in oral drug delivery. *Expert Opin Drug Deliv* 2011;8:1009–1023.

- [24] Sungthongjeen S, Sriamornsak P, Pitaksuteepong T, et al. Effect of degree of esterification of pectin and calcium amount on drug release from pectin-based matrix tablets. *AAPS PharmSciTech* 2004;5:50–57.
- [25] Sriamornsak P, Thirawong N, Puttipipatkachorn S. Emulsion gel beads of calcium pectinate capable of floating on the gastric fluid: effect of some additives, hardening agent or coating on release behavior of metronidazole. *Eur J Pharm Sci* 2005;24:363–373.
- [26] Thirawong N, Nunthanid J, Puttipipatkachorn S, et al. Mucoadhesive properties of various pectins on gastrointestinal mucosa: an in vitro evaluation using texture analyzer. *Eur J Pharm Biopharm* 2007;67:132–140.
- [27] Sriamornsak P, Nunthanid J. Calcium pectinate gel beads for controlled release drug delivery: I. Preparation and in vitro release studies. *Int J Pharm* 1998;160:207–212.
- [28] Sriamornsak P, Nunthanid J, Wanchana S, et al. Composite film-coated tablets intended for colon-specific delivery of 5-aminosalicylic acid: using deesterified pectin. *Pharm Dev Technol* 2003;8:311–318.
- [29] Wong TW, Colombo G, Sonvico F. Pectin matrix as oral drug delivery vehicle for colon cancer treatment. *AAPS PharmSciTech* 2011;12:201–214.
- [30] Sriamornsak P, Niratisai S, Cheewatanakornkool K. Synthesis and characterization of thiolated pectin and pectin-doxorubicin conjugates. The 26th Federation of Asian Pharmaceutical Associations (FAPA) Congress, Bangkok, Thailand, 2016.
- [31] El-Gibaly I. Oral delayed-release system based on Zn-pectinate gel (ZPG) microparticles as an alternative carrier to calcium pectinate beads for colonic drug delivery. *Int J Pharm* 2002;232:199–211.
- [32] Jung J, Arnold RD, Wicker L. Pectin and charge modified pectin hydrogel beads as a colon-targeted drug delivery carrier. *Colloids Surf B Biointerfaces* 2013;104:116–121.
- [33] Sriamornsak P, Nunthanid J, Cheewatanakornkool K, et al. Effect of drug loading method on drug content and drug release from calcium pectinate gel beads. *AAPS PharmSciTech* 2010;11:1315–1319.
- [34] Manchun S, Cheewatanakornkool K, Dass CR, et al. Novel pH-responsive dextrin nanogels for doxorubicin delivery to cancer cells with reduced cytotoxicity to cardiomyocytes and stem cells. *Carbohydr Polym* 2014;114:78–86.
- [35] Rana S, Gallo A, Srivastava RS, et al. On the suitability of nanocrystalline ferrites as a magnetic carrier for drug delivery: functionalization, conjugation and drug release kinetics. *Acta Biomater* 2007;3:233–242.
- [36] Izadi Z, Divsalar A, Saboury AA, et al.  $\beta$ -Lactoglobulin-pectin nanoparticle-based oral drug delivery system for potential treatment of colon cancer. *Chem Biol Drug Des* 2016;88:209–216.
- [37] Korsmeyer RW, Gurny R, Doelker E, et al. Mechanisms of solute release from porous hydrophilic polymers. *Int J Pharm* 1983;15:25–35.
- [38] Higuchi T. Mechanism of sustained-action medication. Theoretical analysis of rate of release of solid drugs dispersed in solid matrices. *J Pharm Sci* 1963;52:1145–1149.
- [39] Huanbutta K, Nernplod T, Akkaramongkolporn P, et al. Design of porous Eudragit<sup>®</sup> L beads for floating drug delivery by wax removal technique. *Asian J Pharm Sci* 2017;12:227–234.
- [40] Grant GT, Morris ER, Rees DA, et al. Biological interactions between polysaccharides and divalent cations: the egg-box model. *FEBS Lett* 1973;32:195–198.
- [41] Assifaoui A, Lerbret A, Uyen HTD, et al. Structural behaviour differences in low methoxy pectin solutions in the presence of divalent cations ( $\text{Ca}^{2+}$  and  $\text{Zn}^{2+}$ ): a process driven by the binding mechanism of the cation with the galacturonate unit. *Soft Matter* 2015;11:551–560.
- [42] Puranik AS, Pao LP, White VM, et al. In vitro evaluation of pH-responsive nanoscale hydrogels for the oral delivery of hydrophobic therapeutics. *Ind Eng Chem Res* 2016;55:10576–10590.
- [43] Abdekhodaie MJ, Liu Z, Erhan SZ, et al. Characterization of novel soybean-oil-based thermosensitive amphiphilic polymers for drug delivery applications. *Polym Int* 2012;61:1477–1484.
- [44] Kalaria DR, Sharma G, Beniwal V, et al. Design of biodegradable nanoparticles for oral delivery of doxorubicin, in vivo pharmacokinetics and toxicity in rat. *Pharm Res* 2009;26:492–501.
- [45] Anbharasi V, Cao N, Feng SS. Doxorubicin conjugated to D- $\alpha$ -tocopheryl polyethylene glycol succinate and folic acid as a prodrug for targeted chemotherapy. *J Biomed Mater Res A* 2010;94A:730–743.
- [46] Cao Y, Gu Y, Ma H, et al. Self-assembled nanoparticle drug delivery systems from galactosylated polysaccharide-doxorubicin conjugate loaded doxorubicin. *Int J Biol Macromol* 2010;46:245–249.
- [47] Timin AS, Lepik KV, Muslimov AR, et al. Intracellular redox induced drug release in cancerous and mesenchymal stem cells. *Colloids Surf B Biointerfaces* 2016;147:450–458.